Optics Letters

Sub-30-fs high-power laser based on a solid multi-pass cell and application for high flux high harmonic generation

Chao Du,[1,2] Hao Teng,[1,2,3,*] Pinbin Li,[1,4] Xiaodong Shao,[1,2] Chengzhi Li,[1,2] Dongliang Wang,[1,2] Baichuan Xie,[1,2] Fabio Frassetto,[5] Luca Poletto,[5] Yan He,[1,2] Jiangfeng Zhu,[4] Chenxia Yun,[1] and Zhiyi Wei[1,2,3,4,6]

[1]Beijing National Laboratory for Condensed Matter Physics and Institute of Physics, Chinese Academy of Sciences, Beijing 100190, China
[2]University of Chinese Academy of Sciences, Beijing 100049, China
[3]Songshan Lake Materials Laboratory, Dongguan 523808, China
[4]School of Optoelectronic Engineering, Xidian University, Xi'an 710071, China
[5]National Research Council—Institute for Photonics and Nanotechnologies, via Trasea 7, I-35131 Padova, Italy
[6]zywei@iphy.ac.cn
*hteng@iphy.ac.cn

Received 18 November 2025; revised 30 January 2026; accepted 6 February 2026; posted 9 February 2026; published 27 February 2026

A multi-pass cell (MPC) serves as a highly effective post-compression solution; however, conventional solid MPC can only accept incident laser pulses with relatively low energy and moderate power. In this Letter, an improved water-cooled solid MPC is introduced for pulse compression of a 186 W high-power femtosecond Yb fiber laser at a 1 MHz repetition rate. Pulse duration of 225 fs is compressed down to 28.3 fs with 161 W output power, which corresponds to a peak power of 5.35 GW. Due to the high peak power, the system was applied to drive high-order harmonics generation (HHG), the XUV light spanned from 20.47 eV to 46.95 eV, with a maximum photon flux up to 1.07×10^{11} photons/s, which is conducive to the application of time-resolved photoemission spectroscopy.

https://doi.org/10.1364/OL.584257

Time-resolved angle-resolved photoemission spectroscopy (Tr-ARPES) has a unique time-resolved and momentum-resolved ability to study the electronic structure in materials [1]. It is now widely applied to the study of unconventional superconductors [2], topological materials [3], charge-density-wave systems [4], and other quantum materials [5]. In recent years, with the great progress of high-order harmonic generation (HHG) driven by fs laser pulse, it has been proven to be a very suitable extreme ultraviolet (XUV) light source for photoemission spectroscopy [6], which has extensive applications in the research of materials containing crucial electronic structures at the point of large momentum [7]. The XUV light source based on high repetition rate (MHz) HHG has many advantages, such as increasing XUV photon flux, improving signal-to-noise ratio [8], and avoiding the space-charge effect [6].

Compared with the Ti:Sapphire laser, Yb-doped laser can operate with average power of kilowatt-level at high repetition rate by adopting both thin-disk amplification scheme [9] and fiber amplification [10]. Therefore, high-power Yb lasers are one of the best driving lasers for achieving high-flux HHG. Driving HHG requires a laser focal intensity exceeding 10^{13} W/cm^2. Achieving this threshold necessitates either higher pulse energy or a shorter pulse duration. Increasing pulse energy typically requires multi-stage amplifiers or coherent beam combination in fiber systems, which adds complexity and cost [11,12]. In contrast, reducing the pulse duration is often a more effective approach. Consequently, achieving a tenfold compression in pulse duration is typically easier than obtaining a tenfold increase in pulse energy.

Efficient pulse compression of high-power Yb-doped fiber lasers is now a major research topic. The basic idea of post-compression is to first broaden the laser spectrum via self-phase modulation (SPM) when the pulse propagates through a transparent nonlinear medium, then the spectrally broadened pulse is compressed by chirped mirrors, resulting in a significantly shorter pulse. Common post-compression schemes include multiple thin plates (MTP) [13,14], hollow-core fiber (HCF) [15,16], and multi-pass cell (MPC) [17–29]. Among these schemes, MPC is particularly effective because it can tolerate high-power and high-energy of incident pulses while also offering high transmission efficiency and excellent beam-pointing tolerance. A typical MPC is configured as a Herriott cell, which consists of two concave mirrors and transparent nonlinear medium placed inside the cavity.

Gas-filled MPC utilizes noble gases such as Neon, Argon, Krypton, and Xenon as nonlinear media. This configuration enables more homogeneous SPM process, minimizes the optical losses, and allows nonlinear compression at high pulse energy. The gas-filled MPC was first introduced in 2018 [17], where 7 bar of Argon was used to compress 275 fs pulses

Corrected 2 March 2026

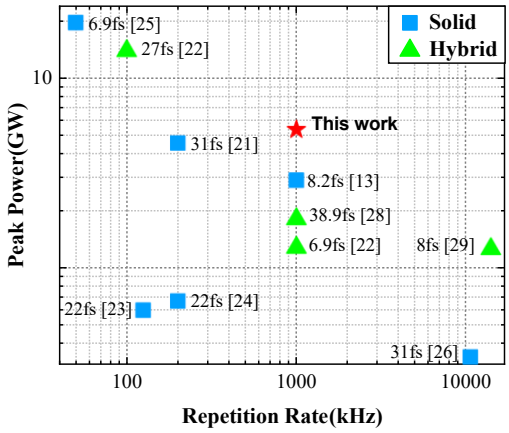

Fig. 1. Overview of the solid-state and solid-gas hybrid MPC compression results at 1030 nm with pulse duration <50 fs and at repetition rate >50 kHz.

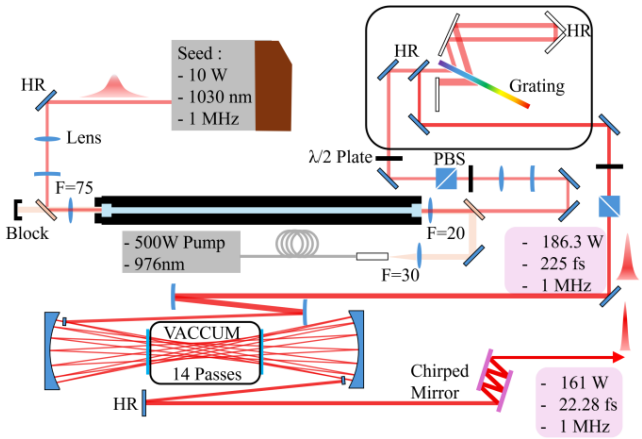

Fig. 2. Schematic setup of the fiber laser system and the solid-plate MPC. (HR, high-reflection mirror; PBS, polarizing beam splitter). The MPC concave mirrors are coated with >99.9% reflectivity at wavelength 950 nm to 1150 nm, and the fused-silica plates are coated with high transmission at the same wavelength range.

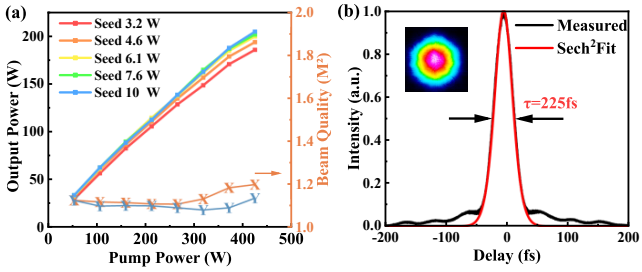

Fig. 3. The characterization measurement of rod-fiber amplifier and compressed pulses. (a) Amplified output power (left axis) and beam quality factor M^2 (right axis) as functions of the pump power. (b) Temporal measured by autocorrelator.

down to 33 fs, which corresponds to a 3.25 GW peak power. Promising progress has been made using first-order helical Laguerre–Gaussian mode to compress the pulses from Yb:YAG thin-disk amplifier (112 mJ, 1.3 ps) to 37 fs at 5 kHz repetition rate [18]. Few-cycle pulses were demonstrated using double-stage gas- filled MPC, where 260 fs were compressed to 5.8 fs (1.7 cycles), corresponding to 173 GW peak power [19].

In 2016, the solid MPC was demonstrated for the first time by Schulte, *et al.* [20]. Since then, much shorter pulses with higher peak power have been realized with solid MPC. For instance, a single stage solid MPC compressed 300 fs 170 μJ Yb laser down to 31 fs, 150 μJ at 200 kHz repetition rate, corresponding to a peak power of 4.5 GW [21]. In 2023, a peak power of 2.9 GW was achieved at 1 MHz using a double-stage solid MPC, which compressed 128 μJ pulses from 1 ps to 8.2 fs with an efficiency of 44% [13]. Similarly, a hybrid scheme comprising a solid MPC followed by an 8.6-bar argon-filled MPC was demonstrated [22]. This system compressed 230 fs pulses to 6.9 fs, delivering 10 μJ of energy at a 1 MHz repetition rate, which corresponds to a peak power of 1 GW. In single Yb rod-fiber amplifier configuration, a gas-filled MPC with 3 bar of Krypton was used to achieve a compression from 240 fs to 35 fs with a pulse energy of 186 μJ at 1 MHz repetition rate [30]. Solid-state MPC still holds great potential for further power scaling, with a good beam quality and system simplicity.

Figure 1 summarizes solid-state and solid-gas hybrid MPC compression results for Yb lasers with pulse duration <50 fs and repetition rate >50 kHz.

In this Letter, we demonstrate a compact, cost-efficient laser system that delivers sub-30-fs, high-power 1030 nm laser based on an improved solid plate MPC and a home-made rod-fiber amplifier at repetition rate of 1 MHz, which was used to generate high flux HHG XUV light source for ARPES. The complete system layout is illustrated in Fig. 2. The amplifier delivers 186.3 W of average power with pulse duration of 225 fs at 1 MHz. A novel water-cooled solid MPC is employed to compress pulses from 225 fs to 28.3 fs, corresponding to a compression ratio of 8, while maintaining the output power of 161 W, with a total transmission efficiency of 86%. The compressed laser pulses attain a peak power of 5.35 GW. To our knowledge, this represents the highest peak power reported for only one stage of solid MPC published at such a high repetition rate, as shown in Fig. 1. The HHG spectral spans from 20.47 eV to 46.95 eV, and maximum flux of single order harmonic reaches 1.07×10^{11} photons/s.

The laser system is a typical fiber chirped-pulse amplification (FCPA) architecture, as shown in Fig. 2. The front end (Huaray laser) provides laser pulses with power of 10 W at repetition rate of 1 MHz. These pulses are stretched to 500 ps by dispersion-tunable chirped fiber Bragg grating (CFBG) and serve as seed pulses for rod-fiber amplifier. The rod-fiber amplifier employs Yb-doped large-mode-area photonic crystal fiber (NKT, aero-GAIN ROD 3.1), whose mode-field diameter exceeds 65 μm ($1/e^2$). A wavelength-stabilized pump laser operating at 976 nm provides up to power of 530 W. The pump laser is coupled into the rod fiber using a fused silica lens with a focal length of 20 mm. Figure 3(a) plots the amplified output power (left axis) and beam quality under 7.6 W seed (right axis) against pump power. The output power increases linearly with pump power until it approaches saturation for pump powers exceeding 400 W. With increase of pump power, the beam quality (M^2) maintains <1.2, which is good due to the rod fiber operating consistently in a single mode. However, when the pump power was further increased beyond 424 W, the thermal effect ultimately limited further power scaling by deteriorating the laser spot quality. Thus, the maximum pump power was set at 424 W, resulting in a maximum amplified output power of 202 W. The amplified laser

pulses, after polarization optimization through a combination of half-wave plate and PBS, are injected into the compressor. The compressor is typically Treacy grating-pair configuration, which has one single transmission grating with line density of 1740 line/mm, and the compression is achieved for input laser passes through the grating four times by right-angle reflective mirrors. After optimization of dispersion compensation between the grating compressor and CFBG stretcher, the compressed pulses were measured to be 225 fs by an autocorrelator (APE-pulsecheck NX50), as shown in Fig. 3(b). The measured autocorrelation trace was fitted by sech^2 function and the sideband of autocorrelation pulse is due to high order dispersion that has not been fully compensated. The compressor delivered an output power of 186.3 W for the 202 W input, which corresponds to a transmission efficiency of 92%.

The post-compression, which is based on the solid plate Herriott-type MPC, is employed for the laser from grating compressor described above. The laser beam is mode-matched through a concave mirror and a convex mirror to the Herriott cell. The MPC consists of two highly reflective mirrors (300 mm radius of curvature) separated by 590 mm. Two 1-mm-thick AR-coated fused silica (Edmund, 11-742) plates serve as nonlinear medium. The two plates are respectively located on both sides about 70 mm away from the focal point of cavity and installed at both ends of a vacuum tube. In order to eliminate thermal effect of plates, the plates are mounted to copper flange, water-cooling is introduced to eliminate the thermal effect of plates. This improved MPC design—featuring in-vacuum plates with active water cooling—effectively mitigates heat accumulation and prevents air-induced filamentation at the intracavity focus.

By optimization of the position of fused silica plates and distance between the cavity of MPC, both strong nonlinear effect and good beam quality are obtained. The radius of spot on the plate is calculated to be 147 μm, the intensity in plate is 2.3×10^{12} W/cm^2, which is below the critical threshold of self-focusing. The beam mode matching in the cavity must be carefully adjusted by measuring the uniformity and size of leakage laser beam from the concave mirror, 14 round trips are chosen for sufficient spectral broadening. The resulting broadened spectrum spans from 980 nm to 1080 nm (Fig. 4(a)), which corresponds to a Fourier-transform-limited pulse duration of 22 fs. Crucially, the nonlinear spectral broadening process did not degrade the beam quality; the output beam maintained a profile with an M^2 factor < 1.3. For dispersion compensation, we used chirped mirrors (UltraFast Innovations, CM39), providing −500 fs^2 of group delay dispersion per bounce over the 980–1080 nm band. By providing −3500 fs^2 compensation, the pulses from the MPC were compressed to a duration of 28.3 fs, as measured by an autocorrelator (APE PulseCheck NX50) and fitted with a sech^2 function (Fig. 4(b)). The system delivers an output power of 161 W, as measured by a high-precision power meter (Ophir FL1100A-BB-65), which corresponds to an overall transmission efficiency of 86%. The measured power exhibited a long-term stability of 0.29% over 6 hours (Fig. 4(c)), which also shows a good stability of pulse energy for HHG.

The specifications from fiber amplifier and MPC are shown in Table 1, and the results show that the compression factor of 8 is realized, and the peak power of laser is enhanced by 7 times, reaching 5.35 GW. This high peak power makes the source an excellent driver for efficient high-harmonic generation.

Figure 5(a) shows the schematic layout of the high-harmonic generation and propagation of XUV beam, including XUV

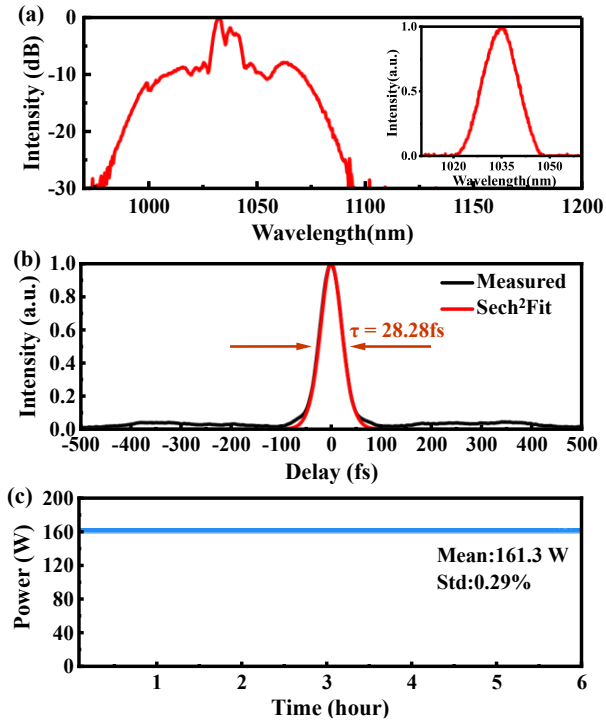

Fig. 4. Characterization of compressed pulse from MPC. (a) The broadening spectral distribution (Log) measured with optical spectrum analyzer (Ando AQ6315A); the inset figure is the incident laser spectrum. (b) Temporal intensity (black solid line) measured by commercial autocorrelator (APE-pulsecheck NX50), sech^2 fit result (red solid line). The main peak includes 90% of the pulse energy. (c) Output power stability in 6 h.

Table 1. Experimental Performance of the Rod-Fiber Laser and Post-Compression

	Amplifier	MPC
τ_{FWHM} (fs)	225	28.28
E (μJ)	186.3	161
P_{avg} (W)	186.3	161
P_{peak} (GW)	0.78	5.35

spectrum distribution measurement and monochromator for selecting of each harmonic. The driving laser (described above) is attenuated by a half-wave plate and a thin-film polarizer (TFP), and focused by a concave mirror (f = 400 mm) into a gas jet to generate HHG. The effective power at the gas target is 134 W. With a measured focal spot diameter of 68.2 μm, the resulting peak intensity is calculated to be 2.44×10^{14} W/cm^2. The HHG beam is collinear with driving laser. A 200 nm-thick Al filter is used to block the driving laser and transmit the HHG to spectrometer. An insertable mirror directs the HHG beam alternately to the XUV flat-field spectrometer or the monochromator. The XUV flat-field spectrometer consists of a gold-coated grating with variable line density and a microchannel plate (MCP) with phosphor screen detector.

By optimization of the gas pressure and gas jet position, the best photon flux was achieved at 1.5 Bar for Kr. The HHG spectrum distribution was measured by an XUV flat-field spectrometer, the typical recorded 2D spectral distribution is presented in Fig. 5(b), and the corresponding intensity profile is

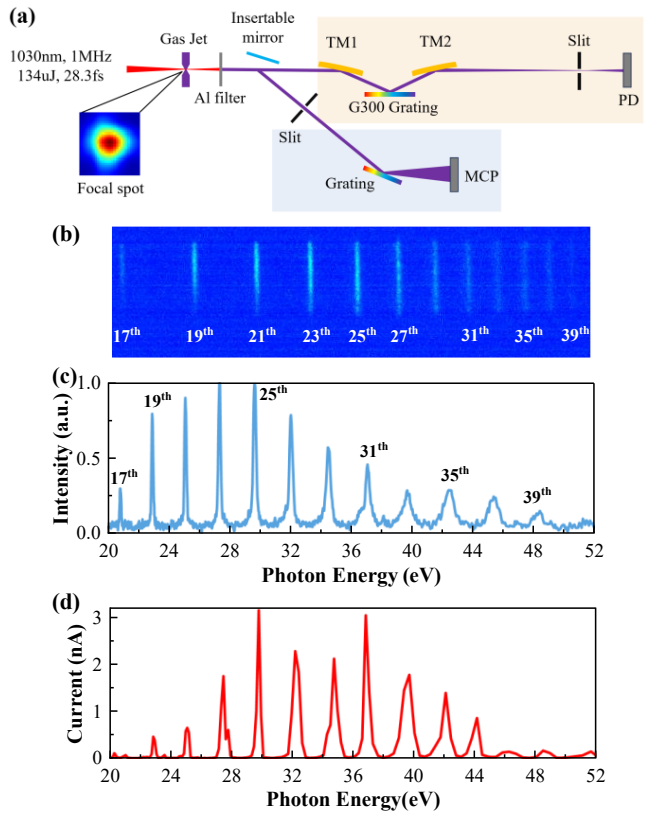

Fig. 5. (a) Schematic setup of the high-harmonic generation and propagation of XUV beam switched to flat-field spectrometer (light blue part) and monochromator (light yellow part) for detecting of each harmonic (MCP, microchannel plate; PD, photodiode; TM, toroidal mirrors). (b) The XUV spectrum 2D distribution measured by flat-field spectrometer. (c) XUV intensity distribution obtained by the spectrometer. (d) XUV spectrum measured by scanning of monochromator with PD.

shown in Fig. 5(c). It spans from 20.47 eV (17th) to 46.95 eV (39th), which is consistent with those of the monochromator, as shown in Fig. 5(d). The strongest flux harmonic is at 30.1 eV (25th). The flux of 25th harmonic was selected by monochromator, collimated by a toroidal mirror, and detected by XUV PD. According to the calibration of the XUV PD, transmission efficiency of the aluminum filter, and the efficiency of the diffraction grating in monochromator (Supplement 1), the maximum photon flux of single harmonic at 30.1 eV is calculated to be 1.07×10^{11} photons/s.

In conclusion, we have developed a home-made, high-power Yb rod-fiber laser system to drive a high-flux tabletop HHG source. The Yb rod-fiber laser delivers an average power of 186 W, corresponding to 225 fs pulses at a repetition rate of 1 MHz. Based on the high-power fs laser, an improved solid plate MPC was developed for spectrum broadening. The MPC design effectively balances strong nonlinear spectral broadening with the preservation of good beam quality. The spectrum was broadened from 980 to 1080 nm and then compressed down to 28.3 fs, which corresponds to a compression factor of 8, and peak power is enhanced to be 5.35 GW. This represents the highest peak power from a single solid plate MPC at 1 MHz repetition rate. Driven by this high peak power laser, the high-order harmonics spanning from 20.47 eV to 46.95 eV are generated. The flux of the isolated 25th harmonic at 30.1 eV was measured to be 1.07×10^{11} photons/s. The results provide an ideal XUV light source for time resolved photoelectron spectrometer.

Funding. National Key R&D Program of China (2022YFA1604200, 2022YFB4601100); National Natural Science Foundation of China (12034020, 12474347, 92250303, 62305373).

Acknowledgment. This work was supported by the Synergetic Extreme Condition User Facility (SECUF).

Disclosures. The authors declare no conflicts of interest.

Data availability. Data underlying the results presented in this Letter are not publicly available at this time but may be obtained from the authors upon reasonable request.

Supplemental document. See Supplement 1 for supporting content.

REFERENCES

1. F. Chen, J. Wang, M. Pan, *et al.*, Rev. Sci. Instrum. **94**, 043905 (2023).
2. A. Damascelli, Z. Hussain, and Z.-X. Shen, Rev. Mod. Phys. **75**, 473 (2003).
3. B. Q. Lv, T. Qian, and H. Ding, Rev. Mod. Phys. **93**, 025002 (2021).
4. P. Chen, Y.-H. Chan, X.-Y. Fang, *et al.*, Nat. Commun. **6**, 8943 (2015).
5. M. Keunecke, C. Möller, D. Schmitt, *et al.*, Rev. Sci. Instrum. **91**, 063905 (2020).
6. M. Puppin, Y. Deng, C. W. Nicholson, *et al.*, Rev. Sci. Instrum. **90**, 023104 (2019).
7. O. Karni, E. Barré, V. Pareek, *et al.*, Nature **603**, 247 (2022).
8. T.-C. Truong, D. Khatri, C. Lantigua, *et al.*, APL Photonics **10**, 040902 (2025).
9. J.-P. Negel, A. Voss, M. Abdou Ahmed, *et al.*, Opt. Lett. **38**, 5442 (2013).
10. T. Eidam, S. Hanf, E. Seise, *et al.*, Opt. Lett. **35**, 94 (2010).
11. Z. Shi, H. Chang, D. Wang, *et al.*, Acta Phys. Sin. **74**, 014205 (2025).
12. J.-S. Wang, Y. Zhang, J.-L. Wang, *et al.*, Acta Phys. Sin. **70**, 034206 (2021).
13. A.-L. Viotti, C. Li, G. Arisholm, *et al.*, Opt. Lett. **48**, 984 (2023).
14. M. Seo, K. Tsendsuren, S. Mitra, *et al.*, Opt. Lett. **45**, 367 (2020).
15. Z. Pi, A. B. Enders, D. Vaso, *et al.*, Opt. Lett. **50**, 4174 (2025).
16. C. Li, K. P. M. Rishad, P. Horak, *et al.*, Opt. Express **22**, 1143 (2014).
17. L. Lavenu, M. Natile, F. Guichard, *et al.*, Opt. Lett. **43**, 2252 (2018).
18. M. Kaumanns, D. Kormin, T. Nubbemeyer, *et al.*, Opt. Lett. **46**, 929 (2021).
19. S. Hädrich, E. Shestaev, M. Tschernajew, *et al.*, Opt. Lett. **47**, 1537 (2022).
20. J. Schulte, T. Sartorius, J. Weitenberg, *et al.*, Opt. Lett. **41**, 4511 (2016).
21. A.-K. Raab, M. Seidel, C. Guo, *et al.*, Opt. Lett. **47**, 5084 (2022).
22. S. Goncharov, K. Fritsch, and O. Pronin, Opt. Lett. **48**, 147 (2023).
23. G. Jargot, N. Daher, L. Lavenu, *et al.*, Opt. Lett. **43**, 5643 (2018).
24. E. Vicentini, Y. Wang, D. Gatti, *et al.*, Opt. Express **28**, 4541 (2020).
25. Y. Liu, Z. Chen, S. Yang, *et al.*, Opt. Lett. **49**, 6992 (2024).
26. S. Gröbmeyer, K. Fritsch, B. Schneider, *et al.*, Appl. Phys. B **126**, 159 (2020).
27. S. Goncharov, K. Fritsch, and O. Pronin, Opt. Lett. **49**, 2717 (2024).
28. M. Seidel, P. Balla, C. Li, *et al.*, Ultrafast Sci. **2022**, 9754919 (2022).
29. A. Omar, M. Hoffmann, G. Galle, *et al.*, Opt. Express **32**, 13235 (2024).
30. D. Wang, Q. Liu, Z. Li, *et al.*, High Power Laser Sci. Eng. **13**, e74 (2025).